

12. NEUTRON STARS

Matthew Baring – Lecture Notes for ASTR 350, Fall 2025

1 Neutron Stars

If the core mass exceeds the Chandrasekhar mass limit during a supernova, then it collapses until another form of degeneracy pressure kicks in to halt collapse. This pressure is **neutron degeneracy pressure**, which can be obtained from the electron version in our white dwarf studies using the substitution $m_e \rightarrow m_n \approx m_p$ in the limit of non-relativistic neutrons:

$$P = \frac{(3\pi^2)^{2/3}}{5} \frac{\hbar^2}{m_p} n_n^{5/3} . \quad (1)$$

C & O,
Sec. 16.6

One can then repeat the hydrostatic analysis. For an $n = 3/2$ polytrope ($\gamma \approx 5/3$) for non-relativistic neutrons, it can be shown that the structure satisfies the fundamental scale for the mass-radius relation:

$$\begin{aligned} R_{\text{ns}} &= 14.64 \left(\frac{\rho_c}{10^{15} \text{ g cm}^{-3}} \right)^{-1/6} \text{ km} \\ M_{\text{ns}} &= 1.102 \left(\frac{\rho_c}{10^{15} \text{ g cm}^{-3}} \right)^{1/2} M_\odot = \left(\frac{15.12 \text{ km}}{R_{\text{ns}}} \right)^3 M_\odot . \end{aligned} \quad (2)$$

The mass-radius relation then becomes

$$M_{\text{ns}} R_{\text{ns}}^3 \propto \frac{1}{m_p^5} \left(\frac{\hbar^2}{G m_p} \right)^3 \text{ i.e., } M_{\text{ns}} R_{\text{ns}}^3 \approx 3.46 M_\odot \left(10 \text{ km} \right)^3 . \quad (3)$$

This implies that neutron stars should have radii on the order of 10^6 cm.

- It then quickly follows that the escape velocity is

$$v_{esc} = \sqrt{\frac{2GM_{ns}}{R_{ns}}} \sim 1.9 \times 10^{10} \text{ cm s}^{-1} = 0.64c . \quad (4)$$

Accordingly, the virial temperatures of neutrons are relativistic, thereby impacting the equation of state. Moreover, general relativity must be incorporated in calculations involving neutron stars.

The choice of $\gamma \approx 5/3$ is quickly justified by forming the neutron dimensionless Fermi momentum parameter:

$$x_n \equiv \frac{p_F}{m_n c} = (3\pi^2 n_n)^{1/3} \frac{\hbar}{m_n c} = 0.548 \left(\frac{\rho}{10^{15} \text{ g cm}^{-3}} \right)^{1/3} \quad (5)$$

If one then forms the mean density for a neutron star,

$$\bar{\rho} = \frac{3M}{4\pi R^3} = 4.75 \times 10^{14} \frac{M}{M_\odot} \left(\frac{R}{10^6 \text{ cm}} \right)^{-3} \text{ g cm}^{-3} , \quad (6)$$

then one infers that for most of the star outside the core, the *neutrons are at most mildly-relativistic*, and often almost non-relativistic. More particularly, the *mean density is of the scale of nuclear densities*.

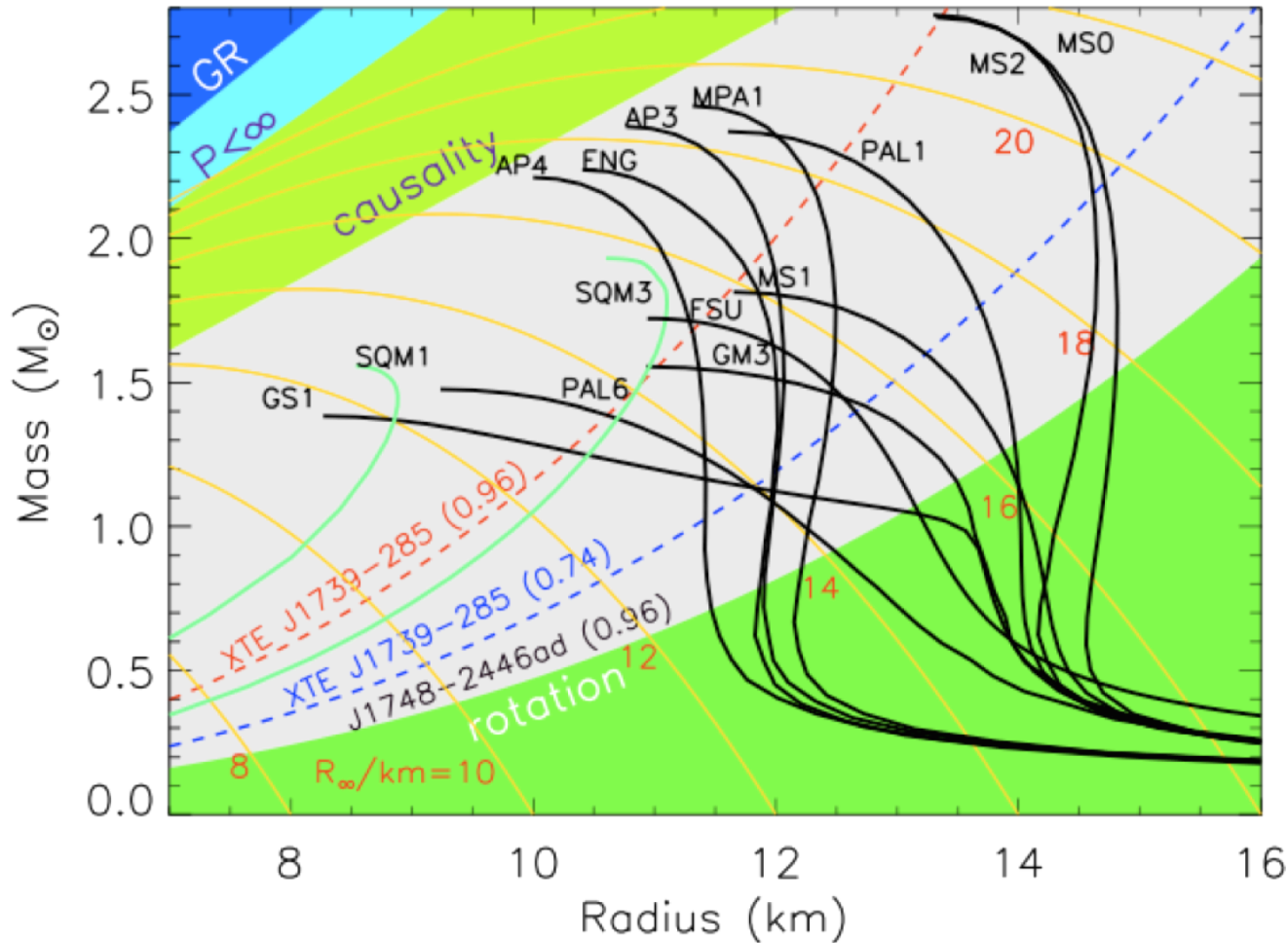
- The mass-radius relation as derived is an over-simplification. In reality, the complexities of the constituents of the stellar interior are (a) very uncertain, and (b) lead to a wide variety of neutron star equations of state (EOS), which (c) then lead to strong departures from the ideal $M_{ns}R_{ns}^3 = \text{constant}$ form.

Plot: Neutron Star Mass-Radius Relation: a Plethora of Models [2]

- Since the electron mass does not appear in the expression for the Chandrasekhar mass limit, an equivalent limit for neutron stars must be of the same order of magnitude. Incorporating an appropriate neutron star equation of state, *the upper bound to neutron star masses* is around $3.2M_\odot$.
- Neutron Stars were predicted by Baade and Zwicky¹ in 1934; they were not conclusively discovered until 1967 in the form of pulsars.

¹Proc. Natl Acad. Sci. USA, **20**, 254 and 259 (1934).

Neutron Star Mass-Radius Relations



- Various NS interior models in the mass-radius plane; from [Lattimer & Prakash \(2007, Phys. Rep. **442**, 109\)](#).
- Observational constraints for 3 neutron stars are depicted.

- The relativistic temperatures and Fermi energies, and high densities, interior to neutron stars effectively drive the neutron/proton equilibrium

$$p + e^- \leftrightarrow n + \nu_e \quad (7)$$

to the rapid production of neutrons. This leads to the **neutronization** of elements heavier than iron (e.g. $^{66}_{28}Ni$ and $^{118}_{36}Kr$), and eventually leads to free neutrons (**neutron drip**) deep in the stellar interior.

Plot: Neutronization Onset

- At what ρ does neutronization occur? Neglecting the neutrino energy, then the energy relation corresponding to Eq. (7) at threshold is

$$\frac{m_e c^2}{\sqrt{1 - v_e^2/c^2}} + m_p c^2 = m_n c^2 \quad , \quad (8)$$

for relativistic electrons, but non-relativistic protons and neutrons. This inverts to the mildly-relativistic result

$$\frac{v_e}{c} = \left\{ 1 - \left(\frac{m_e}{m_n - m_p} \right)^2 \right\}^{1/2} \approx 0.919 \quad . \quad (9)$$

Electron degeneracy and Heisenberg's uncertainty principle then yield

$$\frac{v_e}{c} = \frac{p_e}{m_e c} \sim \frac{\hbar}{m_e c} n_e^{1/3} = \frac{\hbar}{m_e c} \left(\frac{Z}{A} \frac{\rho}{m_p} \right)^{1/3} \quad . \quad (10)$$

Combining and inverting then gives (for $A/Z \sim 1$)

$$\rho \sim m_p \left(\frac{m_e c}{\hbar} \right)^3 \left\{ 1 - \left(\frac{m_e}{m_n - m_p} \right)^2 \right\}^{3/2} \sim 2.3 \times 10^7 \text{ g cm}^{-3} \quad . \quad (11)$$

At this density, encountered very near the surface, *the Fermi energies of protons and neutrons are non-relativistic*, so that a $P \propto \rho^{5/3}$ EOS is operable.

- The **neutronization phase transition** requires energy, which saps the pressure, and so **softens** the EOS to almost $P \propto \rho^0$. The energy comes from gravitational contraction due to declining pressure support.

Plot: Ideal $n - p - e$ Equation of State

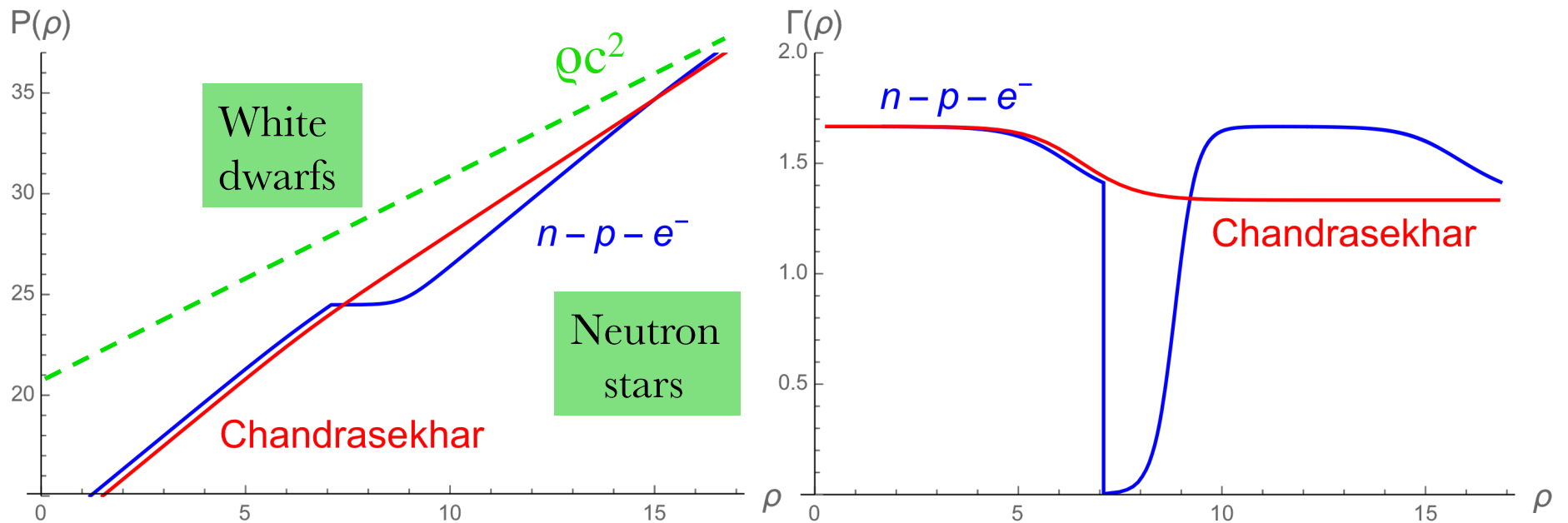
Critical Densities for Onset of Neutronization

	Neutronization Threshold ^a (MeV)	ρ_0 (g cm ⁻³)
${}_1^1\text{H} \rightarrow \text{n}$	0.782	1.22×10^7
${}_2^4\text{He} \rightarrow {}_1^3\text{H} + n \rightarrow 4n$	20.596	1.37×10^{11}
${}_6^{12}\text{C} \rightarrow {}_5^{12}\text{B} \rightarrow {}_4^{12}\text{Be}$	13.370	3.90×10^{10}
${}_8^{16}\text{O} \rightarrow {}_7^{16}\text{N} \rightarrow {}_6^{16}\text{C}$	10.419	1.90×10^{10}
${}_{10}^{20}\text{Ne} \rightarrow {}_9^{20}\text{F} \rightarrow {}_8^{20}\text{O}$	7.026	6.21×10^9
${}_{12}^{24}\text{Mg} \rightarrow {}_{11}^{24}\text{Na} \rightarrow {}_{10}^{24}\text{Ne}$	5.513	3.16×10^9
${}_{14}^{28}\text{Si} \rightarrow {}_{13}^{28}\text{Al} \rightarrow {}_{12}^{28}\text{Mg}$	4.643	1.97×10^9
${}_{16}^{32}\text{S} \rightarrow {}_{15}^{32}\text{P} \rightarrow {}_{14}^{32}\text{Si}$	1.710	1.47×10^8
${}_{26}^{56}\text{Fe} \rightarrow {}_{25}^{56}\text{Mn} \rightarrow {}_{24}^{56}\text{Cr}$	3.695	1.14×10^9

^aFrom Wapstra and Bos (1977); the electron rest mass-energy, $m_e c^2 = 0.511$ MeV, has been subtracted off.

- Neutronization thresholds and corresponding densities. Positive energy is the price of inverse beta decay to increase neutron content => **high for He, low for H.**

Chandrasekhar and Ideal n-p-e⁻ Equations of State



- *Left panel*: Equations of state for the totally degenerate electron **Chandrasekhar** model and the ideal **n-p-e⁻** equilibrium degenerate gas mixture. The **n-p-e⁻** gas pressure at white dwarf (low) densities includes the proton contribution. The pressure is in dyne cm^{-2} and the density is in g cm^{-3} . *Right panel*: The corresponding adiabatic indices. The drop in index Γ with the onset of neutronization at $\sim 10^7 \text{ g cm}^{-3}$ is very prominent.

1.1 Neutron Star Structure

- Neutron decay is suppressed since the high density renders them effectively bound by nuclear forces. In neutron star cores, the composition is unknown ... it may be pure neutrons, or a pion condensate, or a quark superfluid. The central composition is at the core of focal probes of the equation of state (EOS). Different compositions generate different neutrino loss rates.
- The high interior density drives the neutrons to couple as pairs of neutrons, losing Fermionic character and becoming **bosons**. This resembles Cooper-pairing in superconductors.
 - * Since the Pauli exclusion principle does not apply to bosons, all neutron pairs can occupy the ground state. The fluid can therefore lose no energy (e.g. through friction), and so possesses no viscosity – it is a **superfluid**. *Whirlpools/vortices in the superfluid will spin forever!*
- Residual protons down near the core form bosonic pairs that are **superconducting**, i.e. exhibit zero electrical resistance. They can therefore sustain strong magnetic fields.

The interior structure of a neutron star is layered as follows:

The **surface** ($\rho \lesssim 10^6 \text{ g cm}^{-3}$) — a region which may be partially crystalline and even gaseous, wherein temperatures and magnetic fields influence the EOS;

The **outer crust** ($10^6 \text{ g cm}^{-3} \lesssim \rho \lesssim 4.3 \times 10^{11} \text{ g cm}^{-3}$) — a solid region in which a Coulomb lattice of heavy nuclei is in β -equilibrium with a degenerate electron gas. Similar to a white dwarf interior;

The **inner crust** ($4.3 \times 10^{11} \text{ g cm}^{-3} \lesssim \rho \lesssim 2.2 \times 10^{14} \text{ g cm}^{-3}$) — consisting of a lattice of neutron-rich nuclei together with a superfluid neutron gas and an electron gas. Both n and e are degenerate;

The **deep interior** ($2.2 \times 10^{14} \text{ g cm}^{-3} \lesssim \rho \lesssim \rho_{\text{core}}$) — contains superfluid neutrons with a smaller concentration of superfluid protons and electrons;

The **core** ($\rho > \rho_{\text{core}}$) — has neutrons, protons, hyperons, and perhaps a pion condensate and quarks.

- The EOS can be constrained using surface X-ray diagnostics with *Chandra* telescope and Rossi X-ray Timing Explorer (RXTE). For example, the gravitational redshift of any spectral features (e.g. Fe lines) would estimate M/R . In practice, this is very rare: it has not arisen yet.

- * For an ensemble (about 8) of X-ray neutron stars of different ages, the temperature distribution with age can distinguish somewhat between different neutron star models via their predictions of cooling curves.

Plot: Neutron star cooling curves and X-ray temperatures

- * Rampant neutrino emission from high core density scenarios cools neutron stars too fast, conflicting with observations of middle-aged pulsars.

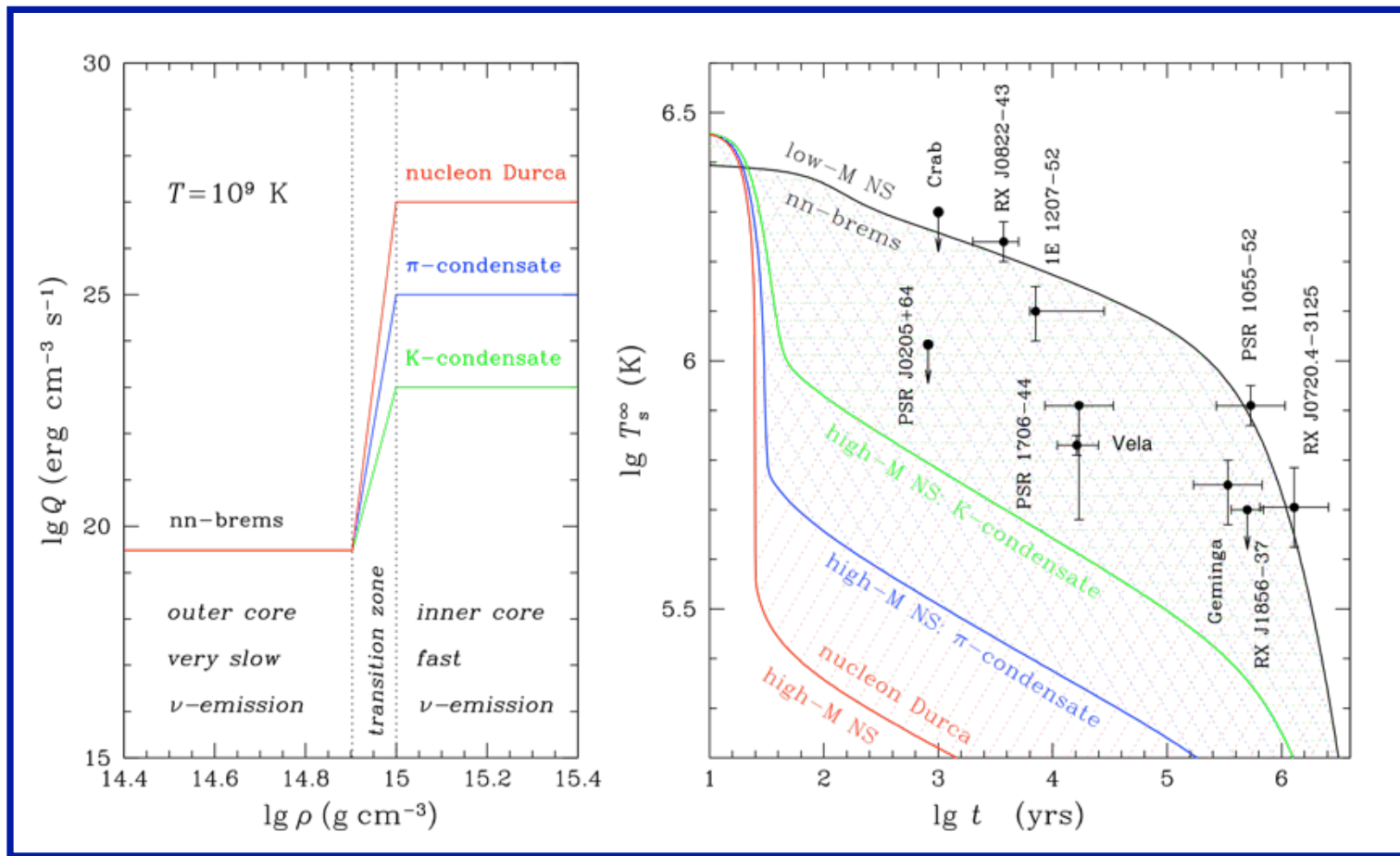
- Interesting M, R diagnostics can be found via different means. If d is known, the Stefan-Boltzmann law gives L and therefore R if the temperature is measured using X-ray spectroscopy with *Chandra*, *XMM-Newton* or *NICER*. This can occasionally be combined with dynamical estimates of M .
- Modeling of precision soft X-ray pulsation light curves of millisecond pulsars by *NICER* yields constraints on M/R in association with general relativistic bending of light emanating from the remote side of the neutron star.

Plot: Dynamical and Other Neutron Star Mass Estimates

- In quasi-edge-on binary systems, gravitational light propagation delays or **Shapiro delay** can probe the mass of the intervening neutron star. A classic example is the millisecond pulsar J1614-2230, illustrating the precision of general relativistic mass determinations.
- Frequencies of **quasi-periodic oscillations** (QPOs) measured by RXTE couple to sound wave/shear wave dynamical timescales R/c_s in surface crustal layers. Inferences of R/c_s can constrain both M and R , and even provide information on the magnetic field strength.

Plot: QPOs in a magnetar light curve power spectrum

Neutron Star Cooling Curves

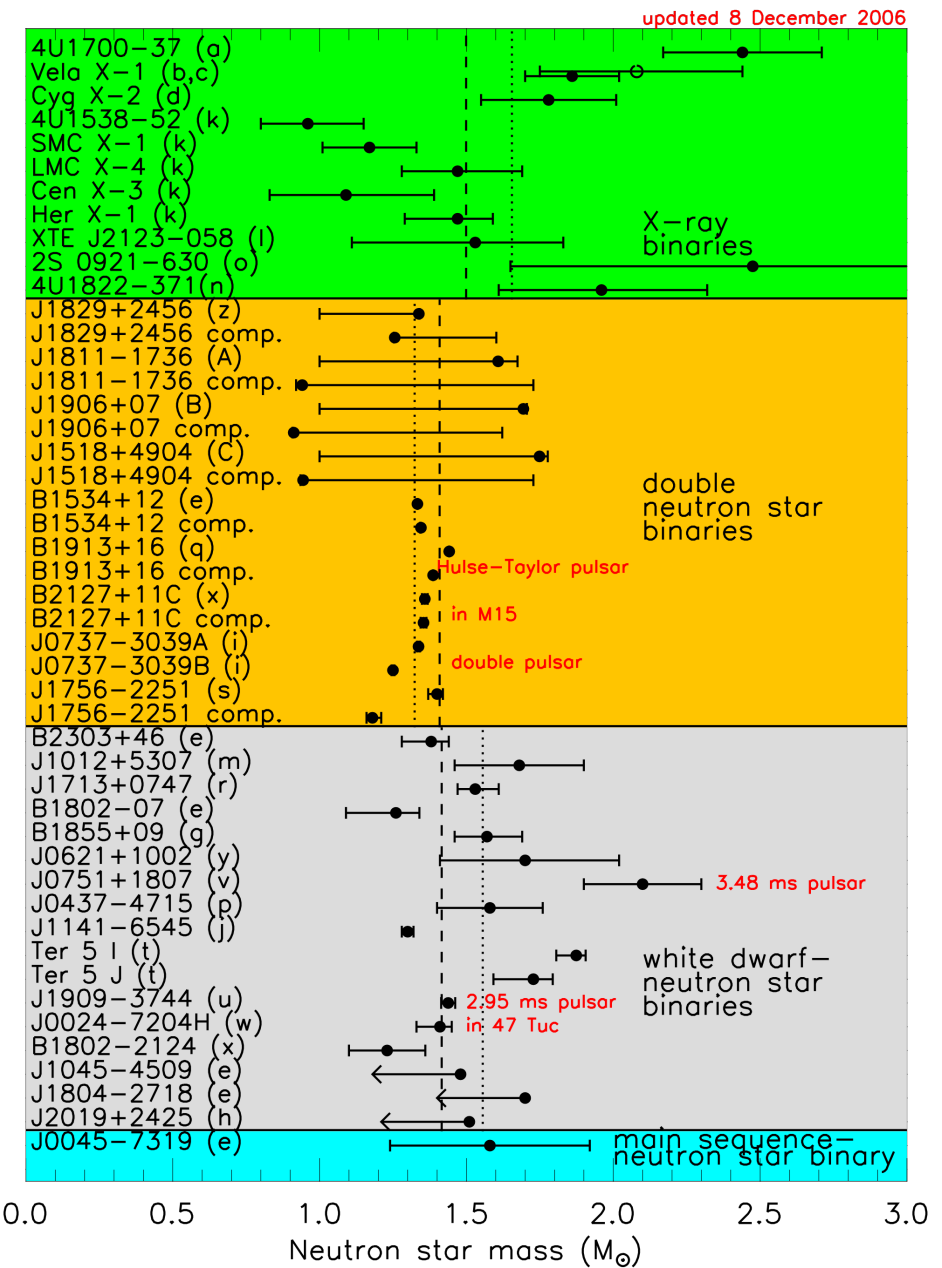


- **Exotic neutron star interiors:** cooling models summarized in [Yakovlev & Pethick \(2004, ARAA 42, 169\)](#).
- **Left:** Schematic density dependence of the neutrino emissivity in a neutron star core at $T = 10^9$ K assuming very slow neutrino emission in the outer core and three scenarios for fast emission in the inner core.
- **Right:** Ranges of T^∞ (single, double and triple hatching) for the three types of fast emission, compared with observations. Each range is limited by the upper cooling curve (low-mass star) and a lower curve (high-mass star).

Observational Bounds on Neutron Star Masses

$$\frac{m_2^3}{(m_1 + m_2)^2} \sin^3 i = \frac{P}{2\pi G} v_{1r}^3 .$$

- Mass constraints of various origins such as dynamical estimates;
- From Lattimer & Prakash (2007, Phys. Rep. 442, 109);
- No NS have definitive mass measurements above 2 solar masses, but...
- See Demorest et al. (2010, Nature 467, 1081) for $1.97M_{\odot}$ Shapiro delay estimate for binary MSP PSR J1614-2230.



Quasi-Periodic Oscillations in the giant flare for SGR 1900+14 of August 27 1998

- Strohmayer & Watts (ApJ 632, L111, 2005): Rossi X-ray Timing Explorer detection of QPOs at **28Hz, 53 Hz, 84Hz** and (main feature) **155Hz**.
- Seen in 1 sec interval only (select rotational phase) of pulsed tail following about 1 minute after initial spike.
- Interpreted as **torsional global seismic oscillations** of crustal ion lattice.
- QPOs seen also in 12/27/04 SGR 1806-20 giant flare tail.

